QM/MM (ONIOM) Study of Glycerol Binding and Hydrogen Abstraction by the Coenzyme B_{12}-Independent Dehydratase

Yuemin Liu,*,† August A. Gallo,† Jan Florián,‡ Yen-Shan Liu,§ Sandeep Mora,§ and Wu Xu*,†

Departments of Chemistry and Chemical Engineering, University of Louisiana at Lafayette, Lafayette, Louisiana 70504 and Department of Chemistry, Loyola University Chicago, Chicago, Illinois 60626

Received: October 29, 2009; Revised Manuscript Received: March 13, 2010

Glycerol binding and the radical-initiated hydrogen transfer by the coenzyme B_{12}-independent glycerol dehydratase from *Clostridium butyricum* were investigated by using quantum mechanical/molecular mechanical (QM/MM) calculations based on the high-resolution crystal structure (PDB code: 1r9d). Our QM/MM calculations of enzyme catalysis considered the electrostatic coupling between the quantum-mechanical and molecular-mechanical subsystems and two alternative mechanisms. In addition to performing QM/MM calculations in the enzyme, we evaluated energetics along the same reaction pathway in aqueous solution modeled by the polarized dielectric and in the virtual enzyme site that included full steric component from the enzyme residues described by molecular mechanics but lacked the electrostatic contribution of these residues. In this way, we established significant enzyme catalytic effect with respect to reference reactions in both an aqueous solution and a nonpolar cavity. Structurally, four hydrogen bonds formed between glycerol and H164, S282, E435, and D447 anchor glycerol for hydrogen abstraction by thiyl radical on C433. These hydrogen-bond partners orient glycerol molecule to facilitate the formation of the transition state for hydrogen abstraction from carbon C1. This reaction then proceeds with the activation free energy of 6.3 kcal/mol and the reaction free energy of 6.1 kcal/mol. The polarization effects imposed by these hydrogen bonds represent a predominant contribution to a 7.5 kcal/mol enzyme catalytic effect. These results demonstrate the importance of electrostatic catalysis and hydrogen-bonding in enzyme-catalyzed radical reactions and advance our understanding of the catalytic mechanism of B_{12}-independent glycerol dehydratases.

Introduction

Glycerol dehydratase (GDH, EC 4.2.1.30) catalyzes the first step of a microbial conversion of glycerol to 1,3-propanediol (1,3-PD) (Scheme 1).[1,2] The transesterification of plant oils and animal fats, which occurs during production of biodiesel as an alternative fuel, yields glycerol as its main byproduct.[3] Since the introduction of the Energy Policy Act of 2005, glycerol generation has been steadily rising. For example, 450 million gallons of biodiesel produced in U.S.A. in 2007 account for 33 million gallons of glycerol. On the other hand, there is an increasing demand for 1,3-PD that can be used in the industrial synthesis of poly(propylene phthalate), a new polyester with unique fiber properties.[1,3,4] Thus, it seems attractive and economically appealing to develop an effective technology that converts glycerol into 1,3-PD.[5]

The chemical conversion of glycerol involves expensive chemicals and toxic intermediates. In contrast, the bacterial conversion of glycerol to 1,3-PD is more environmentally friendly and has a lower cost. Among natural 1,3-PD producers that have been experimentally characterized, there are two major GDH types: coenzyme B_{12}-dependent and B_{12}-independent. To date, several B_{12}-dependent GDHs (e.g., from *Lactobacillus brevis* and *buchnerii*, *Bacillus welchii*, *Citrobacter freundii*, *Klebsiella pneumoniae*, *Clostridium pasteurianum*)[6,7] but only one B_{12}-independent GDH (from *Clostridium butyricum*)[4,8−11] has been identified and investigated in atomic detail. *Clostridium butyricum* has been considered the best natural producer owing to its high yield and titer. In addition, the use of GDH from this bacterial strain does not require a high-cost molecule, vitamin B_{12}, in the culture medium.[4]

Although both classes of GDHs adopt a radical catalytic mechanism, B_{12}-independent GDH differs from its B_{12}-dependent counterpart in that the initial hydrogen abstraction from glycerol is facilitated by a thiyl radical of cysteine 433 (Scheme 1) which is formed after fast radical propagation from 5′-deoxyadenosyl radical of S-adenosylmethionine (SAM) via glycine 763 radical.[12] In contrast, 5′-deoxyadenosyl radical species derived from adenosylcobalamin is directly involved in catalysis in the active site of B_{12}-dependent GDHs.[13] Additionally, presence of potassium ion in the active site of B_{12}-dependent GDH further reinforces active-site differences between the two classes of GDHs.[14] The radical catalytic mechanism appears plausible because the rate constants for model radical reactions in solution are at least 10^8 times larger than rate constants for alternative ionic reactions.[15]

The mechanisms of the radical-involved enzymatic catalysis of B_{12}-dependent GDH and of the related diol dehydratase were studied by experimental and computational methods.[13,14,16−26] In particular, the energy barriers for the hydrogen abstraction by adenosyl radical from the substrate and the hydrogen back-abstraction were computed at the B3LYP/6-31G* level to be 15 and 9.0 kcal/mol, respectively.[25]

The catalytic mechanism for B_{12}-independent GDHs was predicted to be similar to that of its structural homologue from

* Corresponding authors. E-mail: wxx6941@louisiana.edu and yxl3987@louisiana.edu; Tel.: 337-482-5673; Fax: 337-482-5676.

† Department of Chemistry, University of Louisiana at Lafayette.

‡ Department of Chemistry, Loyola University Chicago.

§ Department of Chemical Engineering, University of Louisiana at Lafayette.

10.1021/jp910349q
Published on Web 04/02/2010

SCHEME 1: Proposed Mechanism for the Conversion of Glycerol to 1,3-Propanediol

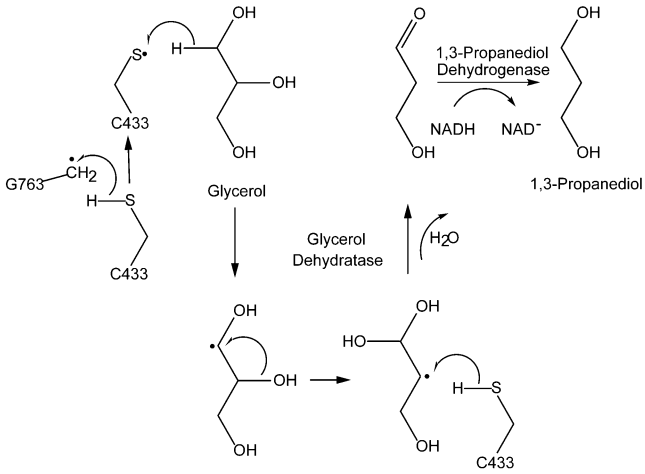

the radical-SAM superfamily−pyruvate formate lyase (PFL).[27] It has been established that formation of a transient thiyl radical represents the initial step for all the glycyl radical enzymes of the radical-SAM superfamily.[28] Thus, in contrast to the initial hydrogen transfer occurring between two carbon atoms in B_{12}-dependent GDH, the hydrogen is abstracted from the glycerol substrate by thiyl radical in B_{12}-independent GDH. Such reaction is likely endothermic because of the low bond-dissociation energy (BDE) of RS-H in organic synthesis[29,30] but is achievable in solution by fine-tuning the BDE of RC-H by functional groups.[31] For example, the rate constant for hydrogen abstraction by cysteamine thiyl radical from thymine C5-CH_3 is $(1.2 \pm 0.8) \times 10^4$ M^{-1} s^{-1}.[32] Computationally, the hydrogen transfer from R−C−H to thiyl radical on cysteine in gas phase was found to be energetically unfavorable with a reaction enthalpy of 19.8−25.7 kcal/mol and an activation energy of 5.97 kcal/mol.[33] A lower reaction enthalpy of 9.7 kcal/mol was calculated for hydrogen abstraction from R−C−H by thiyl radical of Cys79 in class III ribonucleotide reductase,[34] but no theoretical investigations of the catalysis by B_{12}-independent GDHs have been reported.

Thus, in the present study, we employed quantum mechanical/molecular mechanical method (QM/MM),[35] which represents an effective way to study enzymatic catalysis,[36−41] to investigate the initial reaction step in the first step of conversion of glycerol to 1,3-PD—the homolytic cleavage of a CH bond of glycerol by B_{12}-independent GDH from *Clostridium butyricum*. In addition, we analyzed in detail the geometric and energetic aspects of the binding mode of glycerol to this B_{12}-independent GDH.

Methods

QM/MM calculations were carried out by using the structure (PDB code: 1r9d)[27] of glycerol dehydratase with the substrate bound in the active site. The optimization of the geometry of the glycerol B_{12}-independent GDH complex in its ground state (closed shell) and during the hydrogen-transfer reaction (open shell) was carried out by using the ONIOM (B3LYP(UB3LYP for open shell)/6-31G*:Amber) method implemented in the Gaussian 03 program.[42] B3LYP is a density functional method, which consists of the Becke's three-parameter hybrid gradient-corrected exchange functional[43] combined with the gradient-corrected correlation functional of Lee, Yang, and Parr.[44] Although the B3LYP method has a number of well-documented deficiencies,[45] it represents a standard method for QM calculations of organic systems.[46] For example, it has been frequently used for calculations of hydrogen-transfer reactions.[47−49]

B_{12}-independent GDH is a homodimer, which has one independent active site in each of chain A and chain B. The coordinates of chain A of the enzyme with glycerol were extracted for the QM/MM simulation. The 394 water molecules within 3 Å of chain A were included. All the hydrogen atoms were added by using SYBYL program Version 8.0,[50] and the system was subjected to molecular-mechanics optimization. The positions of atoms beyond 15 Å of C2 of glycerol were fixed during the QM/MM simulation.

Adequate treatment of the electrostatic interactions between the QM and MM subsystems has been the most critical issue in the QM/MM simulations.[39] Because no charge embedding was specified in the geometry optimization of the ground-state geometry of the GDH−glycerol complex, a large QM region was applied to alleviate the overpolarization of frontier QM atoms by the link atoms. The link hydrogen atoms were used to saturate the dangling covalent bonds in the QM region.[51,52] This QM region contained a total of 94 atoms including all the side chains of eight residues (i.e., H164, H281, S282, Y339, C433, E435, D447, and Y640) in the active site, eight link hydrogen atoms, glycerol, and one water molecule in the vicinity of D447. The QM regions are further described in detail in Scheme 1 and Table1 in the Supporting Information. The inductive effect introduced from the hosts of link atoms becomes weak at the frontier atoms. The rest of the system was treated with MM by using AMBER force field.[53] The QM and MM regions carried net charges of −2 and −3, respectively, leading to a total net negative charge of −5 for the entire QM/MM system. The whole simulated QM/MM system contained 13 516 atoms.

The intermolecular interaction energies between glycerol and the key residues in the active site of the enzyme were calculated at the B3LYP/6-311++G** method by using the supermolecular approach.[54−57] The influences of solvent were considered by using Tomasi's Polarizable Continuum Model (PCM) with dielectric constants 80, 47, and 4.9, and the Pauling atomic radii were applied for all atoms.[58]

The energy profiles for the hydrogen-transfer pathway from glycerol to the C433 radical in the enzyme were evaluated by single-point QM/MM calculations with full electrostatic embedding of charges of MM region into the Hamiltonian of the QM region, which consisted of 18 atoms of the side chain of C433 and glycerol molecule (small QM region). The geometries for these single-point calculations were obtained by QM/MM calculations using the same QM part but no electrostatic embedding. Because the number of degrees of translational and rotational freedom does not change during hydrogen abstraction in the enzyme active site, the entropic contribution to the activation free energies of both studied hydrogen-transfer reactions is likely to be very small. Thus, the calculated energy changes are assumed to represent free-energy profiles for the studied reactions. The electrostatic potential (ESP) charges and Mulliken spin densities for QM atoms including glycerol were calculated at the B3LYP/6-31G* level.

The free-energy profile for the reference reaction in aqueous solution was calculated by single-point PCM/B3LYP(6-31G*) calculations for the system encompassing the small enzyme−substrate QM region in the geometry optimized in the enzyme active site (see the previous paragraph). The covalent bond of the side chain of the C433 radical that was cut off was terminated with the hydrogen atom. The patched hydrogen atom

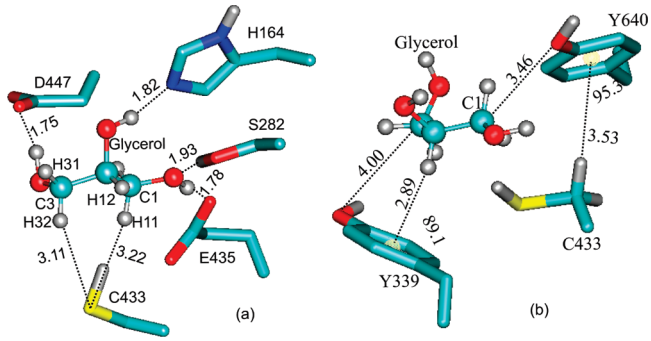

Figure 1. Substrate binding mode in the QM/MM optimized structure. (a) Hydrogen-bond lengths and S···H distances (angstrom). (b) Orientation (degree) and distances (angstrom) of two Tyr residues with respect to glycerol and C433.

TABLE 1: Calculated Contributions of the GDH Active Site Residues to the Glycerol (Gol) Binding Free Energy with the Protein Environment Modeled by Using a Polarized Continuum Described by a Dielectric Constant ε

	ΔG (kcal/mol)[a]		
substrate-residue pair	$\varepsilon = 4.9$	$\varepsilon = 47$	average
Gol−H164	−1.99	−1.52	−1.76
Gol−H281	0.25	0.48	0.37
Gol−S282	−2.28	−1.83	−2.06
Gol−Y339	1.09	1.30	1.20
Gol−C433	2.15	1.53	1.84
Gol−E435	−7.76	−4.02	−5.89
Gol−D447	−2.95	−1.61	−2.28
Gol−Y640	0.86	1.65	1.26
C433−Y339	1.16	1.50	1.33
C433−Y640	0.35	0.57	0.46

[a] PCM/B3LYP/6-311++G** with basis-set superposition error (BSSE) correction.

possessed bond angle and dihedral angle of the host C−C bond. The newly added H−C bond length was optimized at the UB3LYP/6-31G* level for each point of the reaction profile in aqueous solution (with coordinates of all the other atoms fixed).

Results and Discussion

The QM/MM optimized geometry shows the presence of four hydrogen bonds formed between glycerol and the amino acid residues in the enzyme active site (Figure 1a). By using a dielectric constant of 47 to model the screening effect of the protein interior, these hydrogen bonds were calculated to contribute free energies of −1.5, −1.8, −4.0, and −1.6 kcal/mol (for H164N−HO(C2), S282HO−OH(C1), E435O−HO(C1), and D447O−HO(C3), respectively) to the total substrate binding free energy (Table 1). After including also the destabilizing contributions of tyrosine residues (Table 1), the total binding free energy is predicted to fall between −4.0 and −10.6 kcal/mol for the two limiting values of the dielectric constant of 47 and 4.9, respectively. Note that the protein dielectric constant is not a universal constant but simply a parameter that depends on the computational model used to approximate the protein structure and dynamics. This constant usually represents the effect of all the structural factors, such as water penetration or the protein reorganization, that are not considered explicitly.[59,60] Because our theoretical model includes explicitly the interactions of the substrate with the nearby residues but the effects of more distant residues and protein dynamics are treated only implicitly, the actual value of the protein dielectric constant can be expected to fall somewhere between 47 and 4.9. By using the average of the substrate binding free energies calculated with these two limiting values of the protein dielectric, the predicted equilibrium dissociation constant at 298 K is 5 μM. In the absence of experimental dissociation constant or Michaelis constant, K_m, for B_{12}-independent GDH, our prediction appears to fall in a reasonable range when compared with a K_m of 0.5 mM observed for B_{12}-dependent GDH from *C. freundii*.[61]

Although the substrate binding free energy cannot be rigorously decomposed to contributions from individual amino acid residues, it is possible to devise theoretical treatments that provide a physically meaningful free energy decomposition scheme.[62] The applied PCM supermolecular ab initio approach represents one of the possible choices for such decomposition that, in the present case, results in a reasonable dissociation constant.

The fifth hydrogen bond, which was observed in the crystal structure[27] to connect histidine 281 and the hydroxyl group on C2 of glycerol, was not retained in the QM/MM optimized geometry. The two N atoms on the imidazole ring of histidine 281 stay nearly equally (the two N···O distances are 4.46 and 4.48 Å) far away from the O atom at C2 on glycerol. Histidine 281 does not make hydrogen bonds either with other residues in the active site. The discrepancy between the calculated and observed position of histidine 281 side chain may be due to the fact that our simulations were carried out with the thiol form of cysteine 433 rather than its activated thiyl radical form. However, because both forms of the cysteine side chain carry a zero overall charge and this side chain is not involved in hydrogen bonding, the structural consequences of the presence or absence of the additional hydrogen atom should be negligible. Moreover, because the bound glycerol substrate is sufficiently stable in the crystal of the enzyme−substrate complex, it is very likely that also the crystal structure contains the thiol (i.e., nonradical) form of cysteine 433. Unfortunately, at 1.8 Å resolution, it is impossible to conclusively assign the protonation state of the cysteine 433. Despite the absence of a direct hydrogen bond in the ground state, histidine 281 can still play a role in the catalytic transformation of glycerol following initial hydrogen abstraction, as suggested by Lanzilotta and his coworkers.[27]

The two tyrosine residues present in the active site (Figure 1b) may be involved in radical catalysis by GDH, but it is difficult to determine their actual mechanistic role.[63] Interestingly, experimental studies indicated that the aromatic hydrophobic residues render a binding pocket inert to free radical species in radical catalysis.[64] Alternatively, the OH group of one of the tyrosine residues might form a radical hydrogen bonds[65] to stabilize glycerol radical reaction intermediates. Although the short calculated distances of the phenyl rings from the substrate indicate the presence of weak CH-π interactions in the GDH active site, the actual calculated contributions of these two residues to the total substrate binding free energy are positive (Table 1), which indicates that they do not play a role in substrate binding. This view is consistent with the calculated ring orientations that are not among those preferred by CH-π interactions.[66,67]

Hydrogen abstraction represents the initial step of glycerol transformation by GDH (Scheme 1). Binding to GDH generates a prochiral glycerol molecule, in which the two C−H bonds on each of the two ends of the glycerol molecule become distinguishable. The hydrogen atoms H32 (on carbon C3) and H11 (C1) are 3.11 and 3.22 Å away from the sulfur atom of cysteine 433 (Figure 1a). Once the thiyl radical is generated, it is likely to abstract one of these two hydrogen atoms, but the

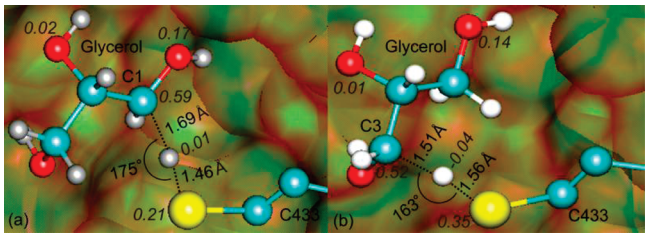

Figure 2. CH and SH bond lengths (angstroms), angle (degrees), and atomic spin densities (a.u.) in the transition state for abstraction of H11 (a) and H32 (b) of glycerol by GDH.

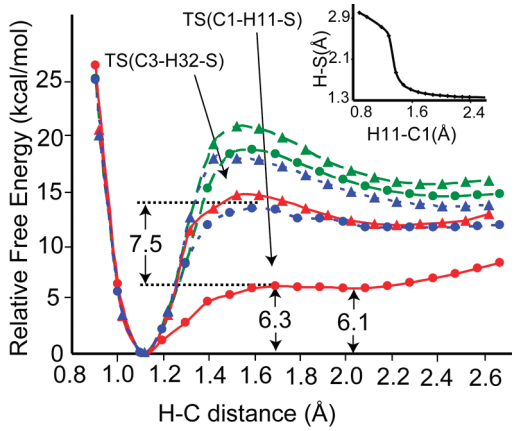

Figure 3. Free energy profiles for hydrogen abstraction from the C1 (●) and C3 (▲) atoms in the enzyme (red, full line), aqueous solution (blue, short dashed line), and nonpolar enzyme (green, long dashed line). The reactions in the nonpolar cavity were modeled by the QM/MM calculations with no embedding of MM charges in the QM Hamiltonian. All free energy profiles by QM/MM were plotted with the total QM/MM energy relative to the total QM/MM energy of the ground state for the hydrogen transfer reaction, which corresponds either to the enzyme−substrate complex with cysteine 433 in its radical form or to the complex of glycerol with cysteine 433 side chain in its radical form in aqueous solution (see also Methods). Arrows labeled 'TS()' indicate the points that correspond to TS geometries shown in Figure 2.

actual preference cannot be deduced by inspecting the ground state structure. Furthermore, the steady- or presteady-state enzyme kinetics data have not yet been published. Therefore, we used QM/MM calculations for the radical-containing enzyme−substrate complex to determine transition state geometries (Figure 2) and free-energy profiles for both possible mechanistic pathways (Figure 3). In addition, in order to evaluate the catalytic effect of the protein environment, we compared these profiles with the energetics of the identical hydrogen-transfer reactions in aqueous solution and in the nonpolar enzyme active site (Figure 3).

The abstraction of H11 by thiyl radical of cysteine 433 is associated with the activation free energy of 6.3 kcal/mol. This free-energy barrier is significantly lower than the barrier for the transfer of H32 (14.7 kcal/mol, Figure 3). Thus, the mechanism involving the transfer of H11 to form a glycerol radical intermediate is predicted to be the preferred initial reaction step. This finding is consistent with the earlier prediction based on the crystal structure.[27] The calculated activation free energy for this reaction step is significantly smaller than the 15 kcal/mol overall barrier for glycerol transformation to 1,3-propanediol estimated from the observed specific activity of GDH from *Clostridium butyricum.* In this estimation, the value of 1.56 mmol min^{-1} mg^{-1}, which was reported by Lanzilotta and his co-workers,[27] was first corrected to a more recent and accurate value of 25 μmol min^{-1} mg^{-1} (W. Lanzilotta, personal communication). In the next step, we converted this specific activity to k_{cat} of 70 s^{-1} by assuming that the catalytically active form of GDH is an activated homodimer with a molecular mass of 175.8 kD, but only one of the two monomers is catalytically active (W. Lanzilotta, personal communication). Finally, we converted this k_{cat} to the activation free energy by using the transition-state theory expression for the temperature of 298 K. The comparison of our calculated activation barrier for the H11 transfer and the estimated experimental barrier for the overall catalytic reaction indicates that the hydrogen-transfer step does not represent the rate-limiting step of the catalytic reaction but a fast pre-equilibrium step.

The free-energy profile of any reaction embodies effects of many structural factors. Although some important factors, for example, the contributions of vibrational energies and entropies, quantum tunneling, or protein dynamics, were neglected in our QM/MM method, other important contributions were examined in detail. In particular, the comparison of the energetics in the enzyme with and without the electrostatic polarization effect of the active-site residues included in the reacting region (Figure 3) may provide important insight into the origin of the catalytic stabilization of the product and transition states for hydrogen transfer by GDH. Additionally, we present analysis of the transition-state geometry and spin density (Figure 2) and the substrate atomic charges in the enzyme and solution (Figure 4).

All the transitional geometries along the reaction coordinate for hydrogen transfer were obtained from QM/MM simulations without charge embedding. Although the no-embedding option represents a default option for the ONIOM calculations in Gaussian 03, the MM region mainly serves as a spatial constraint for QM atoms in these calculations. Thus, the resulting QM/MM energy profile, which effectively approximates free energy due to the negligible entropic contributions (see Methods), represents energetics of a reaction occurring in a nonpolar cavity with the shape of the active site. The energetics of the reaction that did include the polarization effects of the protein environment was mapped out via single-point (i.e., without further optimizing the geometry) QM/MM calculations with charge embedding. Including in these calculations the MM charges into QM Hamiltonian ensures a more realistic picture of the protein environment around the QM region. The comparison of the activation free energies calculated for the substrate−cysteine pair placed in the nonpolar cavity and in the actual electrostatic environment of the protein shows that the electrostatic environment stabilizes the transition-state (TS) structure relative to the ground state by 13.2 kcal/mol for H11 transfer and by 6.5 kcal/mol for H32 transfer. The significant part of this stabilization can probably be attributed to the presence of four hydrogen bonds between glycerol and GDH (Figure 1), although the other polar residues and main-chain dipoles may also contribute to the calculated TS stabilization.

To model the reaction occurring in aqueous solution, the free-energy profile was computed for the small QM cluster containing a side chain of cysteine 433 and a glycerol molecule (denoted as GOL in Figure 3 legend) solvated by using the PCM solvation model with a dielectric constant of 80. To make it comparable to the catalyzed reaction, no further optimizations were done for the geometries extracted from the enzyme. For these geometries, PCM solvation free energies were added as single-point calculations. Employing the nonspecific solvation effects by using the PCM model lowers the activation and reaction free energies for the H11-transfer reaction by 6.0 kcal/mol compared to the reaction in the nonpolar cavity. If we assume that the

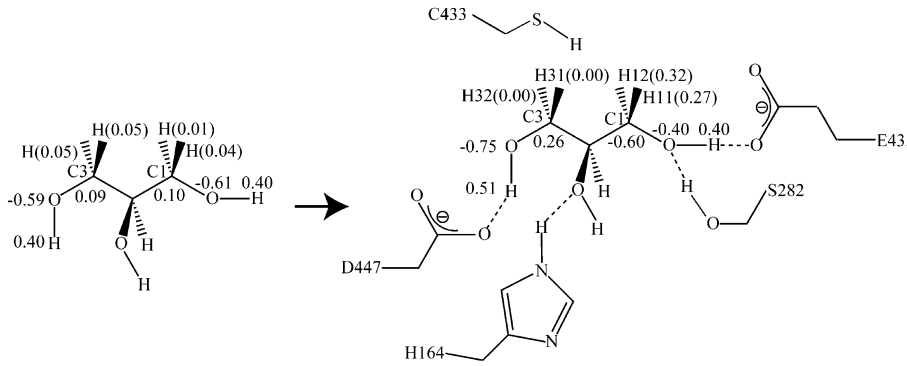

Figure 4. ESP charge distribution of isolated glycerol and glycerol in the QM/MM optimized geometry.

nonspecific solvation effects also contribute about 6 kcal/mol to the TS stabilization in the enzyme, the remaining 7.5 kcal/mol of the 13.5 kcal/mol difference between the activation free energy for H11 transfer in the enzyme and in the nonpolar enzyme cavity can be attributed to the presence of hydrogen-bonding and other specific electrostatic effects from the active -site residues. In contrast, the catalytic effect of the enzyme on the transfer of H32 is only about 4 kcal/mol. Although the transfer of H11 in the enzyme active site is associated with a positive reaction free-energy change (6.1 kcal/mol), this energy is low enough to allow fast substrate turnover if the barriers for the subsequent reaction steps depicted in Scheme 1 are below 10 kcal/mol. Interestingly, our QM/MM reaction free energy of 6.1 kcal/mol is close to the value of 8 kcal/mol that can be obtained by simple subtraction of the experimental bond-dissociation energies of the CH and SH bonds[30] but is significantly less favorable than the value of −1.8 kcal/mol calculated for the initial hydrogen abstraction by B_{12}-dependent GDH.[26]

In an attempt to rationalize the catalytic effect of the enzyme and its different magnitude for H11 and H32 hydrogen-transfer pathways, we calculated ESP-derived atomic charges for the glycerol molecule either solvated by the PCM solvation model or bound in the enzyme active site by the single-point QM/MM with charge embedding (Figure 4). The ESP charges exhibit better performance than other types of charges in reproducing the dipole moment of the molecule.[68,69] The charge (in a.u.) for H32 drops to 0.00 in the enzyme from 0.06 in solution. In contrast, the H11 becomes more positive (0.27 a.u.) upon substrate binding. This difference between H11 and H32 atomic charges in the enzyme indicates that the hydrogen bonds not only play a structural role in anchoring the substrate molecule but also cause a different polarization effect on the C−H bonds at the two ends of the glycerol molecule. The likely reason for these variations is that the electron-donating effect of hydrogen-acceptor (E435) hydrogen bond on C1 is partially canceled by the hydrogen donor (S282), whereas only hydrogen acceptor D447 formed a hydrogen bond with OH on C3. Consequently, differential inductive effects lead to distinct polarizations of the two C−H bonds. The lower electron density on H11 (ESP: 0.27 of H11 vs 0.00 of H32) implies a weaker C−H bond; therefore, the hydrogen H11 on C1 is more easily abstracted by the thiyl radical. This is the case also during the course of hydrogen migration, when the charge of H11 is always 0.1 a.u. higher than that of H32 (Figure 5). The charge effects on the C−H to H−S hydrogen-transfer reactions have been found to be an important factor affecting reaction rates in organic solvents, for which it was proposed that the rate of the radical hydrogen-transfer reaction highly depends on the reactant polar effect and reaction enthalpy.[29] Here, we found that the favorable polarization effects due to the enzyme active site parallel those caused by favorable substituent effects in organic reactions in solution.

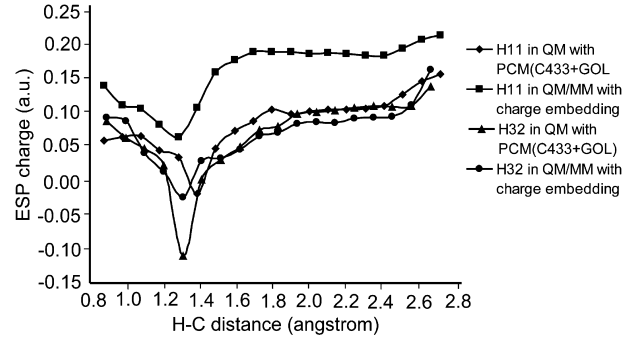

Figure 5. Variation of the charge of the transferring hydrogen during the course of hydrogen abstraction.

Additional factors that may contribute to the catalytic preference for H11 transfer involve a more linear geometry of the C−H11−S atoms in the TS than for the C−H32−S atoms and small differences in the delocalization of the spin density over the glycerol−cysteine pair (Figure 2). However, because these differences exist for a large part already in the TS for the model reaction in solution, their contribution to GDH catalysis is likely negligible in comparison with specific electrostatic effects.

In summary, we carried out a series of QM/MM simulations to investigate the energetics of two alternative mechanisms of the first step of the catalytic transformation of glycerol by the B_{12}-independent GDH of *Clostridium butyricum*. Although the initial hydrogen-transfer reaction step is a radical reaction, we found that specific electrostatic effects provided by the active-site residues significantly lower the activation free energy of this reaction. In addition to performing QM/MM calculations in the enzyme, we also evaluated energetics along the same reaction pathway in the aqueous solution modeled by the polarized dielectric and in the enzyme site that included full steric component from the enzyme residues described by MM but lacked the electrostatic contribution of these residues. In this way, we established significant enzyme catalytic effect with respect to reference reactions in both aqueous solution and nonpolar cavity. Our results indicate that the four hydrogen bonds formed between glycerol and H164, S282, E435, and D447 are employed to orient the glycerol molecule for hydrogen abstraction from carbon C1. Furthermore, polarization effects yielded by these hydrogen bonds dominate the catalytic mechanism of the initial hydrogen abstraction, which represents an example of electrostatic catalysis in a radical reaction. The lower electron density on H11 makes it more likely that the hydrogen abstraction occurs on C1, which is consistent with the prediction

based on the solved crystal structure.[27] This information provides foundation for future enzyme engineering to pursue more catalytically efficient B_{12}-independent GDHs.

Acknowledgment. This work is funded by Information Technology Initiative Grant from the Louisiana State (to W.X. and Y.-S.L.) and by Research Innovation Award from Research Corporation (to J.F.). The authors are grateful to the Dean Mark E. Zappi of College of Engineering and the Dean Bradd Clark of College of Sciences of the University of Louisiana at Lafayette for their supports. We appreciate Nian F. Tzeng's support in providing us computational resources and the g03 program. We also thank William Lanzilotta for helpful suggestions and Itthichok Jangjaimon and Soumik Ghosh for the technical assistance. The QM/MM calculations of B_{12}-independent glycerol dehydratase were conducted with high-performance computational resources provided by the Louisiana Optical Network Initiative (http://www.loni.org).

Supporting Information Available: Parameter data and scheme for the QM region. This material is available free of charge via the Internet at http://pubs.acs.org.

References and Notes

(1) Deckwer, W.-D. *FEMS Microbiol. Rev.* **1995**, *16*, 143.
(2) Liao, D. I.; Dotson, G.; Turner, I., Jr.; Reiss, L.; Emptage, M. *J. Inorg. Biochem.* **2003**, *93*, 84.
(3) Gonzalez-Pajuelo, M.; Andrade, J. C.; Vasconcelos, I. *J. Ind. Microbiol. Biotechnol.* **2004**, *31*, 442.
(4) Gonzalez-Pajuelo, M.; Meynial-Salles, I.; Mendes, F.; Soucaille, P.; Vasconcelos, I. *Appl. Environ. Microbiol.* **2006**, *72*, 96.
(5) Németh, Á.; Sevella, B. *Appl. Biochem. Biotechnol.* **2008**, *144*, 47.
(6) Sobolov, M.; Smiley, K. L. *J. Bacteriol.* **1960**, *79*, 261.
(7) Zhao, Y.-N.; Chen, G.; Yao, S.-J. *Biochem. Eng. J.* **2006**, *32*, 93.
(8) Gonzalez-Pajuelo, M.; Meynial-Salles, I.; Mendes, F.; Andrade, J. C.; Vasconcelos, I.; Soucaille, P. *Metab. Eng.* **2005**, *7*, 329.
(9) Raynaud, C.; Sarcabal, P.; Meynial-Salles, I.; Croux, C.; Soucaille, P. *Proc. Natl. Acad. Sci. U.S.A.* **2003**, *100*, 5010.
(10) Saint-Amans, S.; Girbal, L.; Andrade, J.; Ahrens, K.; Soucaille, P. *J. Bacteriol.* **2001**, *183*, 1748.
(11) Scott, K. P.; Martin, J. C.; Campbell, G.; Mayer, C. D.; Flint, H. J. *J. Bacteriol.* **2006**, *188*, 4340.
(12) Jarrett, J. T. *Curr. Opin. Chem. Biol.* **2003**, *7*, 174.
(13) Golding, B. T.; Radom, L. *J. Am. Chem. Soc.* **1976**, *98*, 6331.
(14) Toraya, T.; Yoshizawa, R.; Eda, M.; Yamabe, T. *J. Biochem.* **1999**, *126*, 650.
(15) Wong, P. C.; Marriott, P. R.; Griller, D.; Nonhebel, D. C.; Perkins, M. J. *J. Am. Chem. Soc.* **1981**, *103*, 7761.
(16) Essenberg, M. K.; Frey, P. A.; Abeles, R. H. *J. Am. Chem. Soc.* **1971**, *93*, 1242.
(17) Moore, K. W.; Bachovchin, W. W.; Gunter, J. B.; Richards, J. H. *Biochemistry* **2002**, *18*, 2776.
(18) Manitto, P.; Speranza, G.; Fontana, G.; Galli, A. *Helv. Chim. Acta* **1998**, *81*, 2005.
(19) George, P.; Glusker, J. P.; Bock, C. W. *J. Am. Chem. Soc.* **1997**, *119*, 7065.
(20) George, P.; Glusker, J. P.; Bock, C. W. *J. Am. Chem. Soc.* **1995**, *117*, 10131.
(21) Brown, K. L.; Marques, H. M. *J. Inorg. Biochem.* **2001**, *83*, 121.
(22) Geremia, S.; Calligaris, M.; Randaccio, L. *Eur. J. Inorg. Chem.* **1999**, *1999*, 981.
(23) Kamachi, T.; Toraya, T.; Yoshizawa, K. *Chemistry* **2007**, *13*, 7864.
(24) Sandala, G. M.; Smith, D. M.; Coote, M. L.; Golding, B. T.; Radom, L. *J. Am. Chem. Soc.* **2006**, *128*, 3433.
(25) Toraya, T.; Eda, M.; Kamachi, T.; Yoshizawa, K. *J. Biochem.* **2001**, *130*, 865.
(26) Eda, M.; Kamachi, T.; Yoshizawa, K.; Toraya, T. *Bull. Chem. Soc. Jpn.* **2002**, *75*, 1469.
(27) O'Brien, J. R.; Raynaud, C.; Croux, C.; Girbal, L.; Soucaille, P.; Lanzilotta, W. N. *Biochemistry* **2004**, *43*, 4635.
(28) Himo, F.; Siegbahn, P. E. M. *Chem. Rev.* **2003**, *103*, 2421.
(29) Roberts, B. P. *Chem. Soc. Rev.* **1999**, *28*, 25.
(30) Luo, Y.-R. *Comprehensive Handbook of Chemical Bond Energies*; CRC Press, 2007.
(31) Himo, F. *Chem. Phys. Lett.* **2000**, *328*, 270.
(32) Nauser, T.; Schoneich, C. *Chem. Res. Toxicol.* **2003**, *16*, 1056.
(33) Rauk, A.; Yu, D.; Armstrong, D. A. *J. Am. Chem. Soc.* **1998**, *120*, 8848.
(34) Cho, K.-B.; Himo, F.; Graslund, A.; Siegbahn, P. E. M. *J. Phys. Chem. B* **2001**, *105*, 6445.
(35) Warshel, A.; Levitt, M. *J. Mol. Biol.* **1976**, *103*, 227.
(36) Warshel, A. *Computer Modeling of Chemical Reactions in Enzymes and Solutions*; John Wiley & Sons, 1991.
(37) Senn, H. M.; Thiel, W. *Curr. Opin. Chem. Biol.* **2007**, *11*, 182.
(38) Gao, J. *Reviews in Computational Chemistry*; VCH: New York, 1992; Vol. 7.
(39) Bentzien, J.; Florián, J.; Glennon, T. M.; Warshel, A. QM/MM approaches for studying chemical reactions in proteins and solution. In *Combined Quantum Mechanical & Molecular Mechanical Methods*; Gao, J., Thompson, M. A., Eds.; American Chemical Society: Washington, DC, 1998; pp 16.
(40) Murphy, R. B.; Philipp, D. M.; Friesner, R. A. *J. Comput. Chem.* **2000**, *21*, 1442.
(41) Field, M. J. *J. Comput. Chem.* **2002**, *23*, 48.
(42) Frisch, M. J.; Trucks, G. W.; Schlegel, H. B.; Scuseria, G. E.; Robb, M. A.; Cheeseman, J. R.; Montgomery, J. A. J.; Vreven, T.; Kudin, K. N.; Burant, J. C.; Millam, J. M.; Iyengar, S. S.; Tomasi, J.; Barone, V.; Mennucci, B.; Cossi, M.; Scalmani, G.; Rega, N.; Petersson, G. A.; Nakatsuji, H.; M. Hada, M. E.; Toyota, K.; Fukuda, R.; Hasegawa, J.; Ishida, M.; Nakajima, T.; Honda, Y.; Kitao, O.; Nakai, H.; Klene, M.; Li, X.; Knox, J. E.; Hratchian, H. P.; Cross, J. B.; Bakken, V.; Adamo, C.; Jaramillo, J.; Gomperts, R.; Stratmann, R. E.; Yazyev, O.; Austin, A. J.; Cammi, R.; Pomelli, C.; Ochterski, J. W.; Ayala, P. Y.; Morokuma, K.; Voth, G. A.; Salvador, P.; Dannenberg, J. J.; Zakrzewski, V. G.; Dapprich, S.; Daniels, A. D.; Strain, M. C.; Farkas, O.; Malick, D. K.; Rabuck, A. D.; Raghavachari, K.; Foresman, J. B.; Ortiz, J. V.; Cui, Q.; Baboul, A. G.; Clifford, S.; Cioslowski, J.; Stefanov, B. B.; Liu, G.; Liashenko, A.; Piskorz, P.; Komaromi, I.; Martin, R. L.; Fox, D. J.; Keith, T.; Al-Laham, M. A.; Peng, C. Y.; Nanayakkara, A.; Challacombe, M.; Gill, P. M. W.; Johnson, B.; Chen, W.; Wong, M. W.; Gonzalez, C.; Pople, J. A. *Gaussian 03*, Revision C.02; Gaussian, Inc.: Wallingford CT, 2004.
(43) Becke, A. D. *J. Chem. Phys.* **1993**, *98*, 5648.
(44) Lee, C.; Yang, W.; Parr, R. G. *Phys. Rev.B.* **1988**, *37*, 785.
(45) Zhao, Y.; Truhlar, D. G. *Acc. Chem. Res.* **2008**, *41*, 157.
(46) Tirado-Rives, J.; Jorgensen, W. L. *J. Chem. Theory Comput.* **2008**, *4*, 297.
(47) Strajbl, M.; Florián, J.; Warshel, A. *J. Phys. Chem. B* **2000**, *77*, 44.
(48) Luzhkov, V. B. *Chem. Phys.* **2005**, *314*, 211.
(49) Kar, T.; Scheiner, S.; Sannigrahi, A. B. *J. Phys. Chem. A* **1998**, *102*, 5967.
(50) SYBYL 7.3; Tripos International: 1699 South Hanley Rd. St. Louis, Missouri, 63144.
(51) Singh, U. C.; Kollman, P. A. *J. Comput. Chem.* **1986**, *7*, 718.
(52) Field, M. J.; Bash, P. A.; Karplus, M. *A combined quantum mechanical and molecular mechanical potential for molecular dynamics simulations*, 1990; Vol. 11; pp 700.
(53) Cornell, W. D.; Cieplak, P.; Bayly, C. I.; Gould, I. R.; Merz, K. M.; Ferguson, D. M.; Spellmeyer, D. C.; Fox, T.; Caldwell, J. W.; Kollman, P. A. *J. Am. Chem. Soc.* **1995**, *117*, 5179.
(54) Wang, Y.; Hu, X. *J. Am. Chem. Soc.* **2002**, *124*, 8445.
(55) Boys, S.; Bernardi, F. *Mol. Phys.* **1970**, *19*, 553.
(56) Mao, L.; Wang, Y.; Liu, Y.; Hu, X. *J. Am. Chem. Soc.* **2003**, *125*, 14216.
(57) Liu, Y.; Hu, X. *J. Phys. Chem. A* **2006**, *110*, 1375.
(58) Cossi, M.; Barone, V.; Cammi, R.; Tomasi, J. *Chem. Phys. Lett.* **1996**, *255*, 327.
(59) Dwyer, J. J.; Gittis, A. G.; Karp, D. A.; Lattman, E. E.; Spencer, D. S.; Stites, W. E.; Garcia-Moreno, E. B. *Biophys. J.* **2000**, *79*, 1610.
(60) Schutz, C. N.; Warshel, A. *Proteins: Struct., Funct. Gen.* **2001**, *44*, 400.
(61) Knietsch, A.; Bowien, S.; Whited, G.; Gottschalk, G.; Daniel, R. *Appl. Environ. Microbiol.* **2003**, *69*, 3048.
(62) Bren, M.; Florián, J.; Mavri, J.; Bren, U. *Theoretical Chemistry Accounts: Theory, Computation, and Modeling (Theoretica Chimica Acta)* 2007, *117*, 535.
(63) Sharma, P. K.; Chu, Z. T.; Olsson, M. H. M.; Warshel, A. *Proc. Natl. Acad. Sci. U.S.A* **2007**, *104*, 9661.
(64) Ormö, M.; Regnström, K.; Wang, Z.; Que, L, Jr.; Sahlin, M.; Sjöberg, B.-M. *J. Biol. Chem.* **1995**, *270*, 6570.
(65) Hammerum, S. *J. Am. Chem. Soc.* **2009**, *131*, 8627.
(66) Bazzicalupi, C.; Dapporto, P. *Struc. Chemistry* **2004**, *15*, 259.
(67) Takahashi, O.; Kohno, Y.; Iwasaki, S.; Saito, K.; Iwaoka, M.; Tomoda, S.; Umezawa, Y.; Tsuboyama, S.; Nishio, M. *Bull. Chem. Soc. Jpn.* **2001**, *74*, 2421.
(68) Clare, B. W.; Supuran, C. T. *J. Mol. Struct.* **1998**, *428*, 109.
(69) Becker, C. F.; Guimarães, J. A.; Verli, H. *Carbohydr. Res.* **2005**, *340*, 1499.

JP910349Q